Journal of South American Earth Sciences 63 (2015) 162–171

Contents lists available at ScienceDirect

Journal of South American Earth Sciences

journal homepage: www.elsevier.com/locate/jsames

Variation of *b* and *p* values from aftershocks sequences along the Mexican subduction zone and their relation to plate characteristics

L. Ávila-Barrientos [a, b, *], F.R. Zúñiga [c], Q. Rodríguez-Pérez [a, c], M. Guzmán-Speziale [c]

[a] Consejo Nacional de Ciencia y Tecnología, Dirección Adjunta de Desarrollo Científico, Mexico
[b] División de ciencias de la Tierra, Departamento de Sismología, Centro de Investigación Científica y de Educación Superior de Ensenada, Baja California, Mexico
[c] Centro de Geociencias, Universidad Nacional Autónoma de México, Querétaro, Mexico

ARTICLE INFO

Article history:
Received 17 February 2015
Received in revised form
1 June 2015
Accepted 8 July 2015
Available online 11 July 2015

Keywords:
Aftershocks
p value
b value
Mexican subduction zone

ABSTRACT

Aftershock sequences along the Mexican subduction margin (between coordinates 110°W and 91°W) were analyzed by means of the *p* value from the Omori–Utsu relation and the *b* value from the Gutenberg–Richter relation. We focused on recent medium to large ($M_w > 5.6$) events considered susceptible of generating aftershock sequences suitable for analysis. The main goal was to try to find a possible correlation between aftershock parameters and plate characteristics, such as displacement rate, age and segmentation. The subduction regime of Mexico is one of the most active regions of the world with a high frequency of occurrence of medium to large events and plate characteristics change along the subduction margin. Previous studies have observed differences in seismic source characteristics at the subduction regime, which may indicate a difference in rheology and possible segmentation. The results of the analysis of the aftershock sequences indicate a slight tendency for *p* values to decrease from west to east with increasing of plate age although a statistical significance is undermined by the small number of aftershocks in the sequences, a particular feature distinctive of the region as compared to other world subduction regimes. The *b* values show an opposite, increasing trend towards the east even though the statistical significance is not enough to warrant the validation of such a trend. A linear regression between both parameters provides additional support for the inverse relation. Moreover, we calculated the seismic coupling coefficient, showing a direct relation with the *p* and *b* values. While we cannot undoubtedly confirm the hypothesis that aftershock generation depends on certain tectonic characteristics (age, thickness, temperature), our results do not reject it thus encouraging further study into this question.

1. Introduction

Aftershocks remain one of the key characteristics of seismicity. Even though many studies have focused on the subject of aftershocks from the time of the first detailed descriptions of the phenomena by Omori (e.g. Omori, 1895), to-date the mechanism behind their generation remains, among other problems unsolved. The analysis of the parameters p of Omori–Utsu relation (Utsu et al., 1995):

$$n(t) = K(t + c)^{-p} \quad (1)$$

where *K* and *c* are constants and *p* is the parameter which control the decay rate, describes the expected number of aftershocks at time t. On the other hand, the Gutenberg–Richter relation (Gutenberg and Ritcher, 1942) be it related to background seismicity or aftershock sequences (relative distribution between large and small events):

$$Log\ N = a - b \cdot M \quad (2)$$

where *N* is the number of earthquakes with magnitude larger or equal to *M*, describes the magnitude distribution for a particular time interval, which can be used for estimation of seismic hazard.

* Corresponding author. División de ciencias de la Tierra, Departamento de Sismología, Centro de Investigación Científica y de Educación Superior de Ensenada, Carretera Ensenada-Tijuana No. 3918, Zona Playitas, C.P. 22860, Ensenada, Baja California, Mexico.
E-mail address: lenavila@cicese.mx (L. Ávila-Barrientos).

http://dx.doi.org/10.1016/j.jsames.2015.07.009
0895-9811/

The heterogeneity of seismicity at aftershock zones has been systematically studied in detail (i.e. Enescu and Ito, 2002; Enescu et al., 2011; Kato and Igarashi, 2012; Kato et al., 2007; Toda et al., 1998; Utsu et al., 1995; Wiemer and Wyss, 2000; Wiemer and Katsumata, 1999). These studies have demonstrated that the activity, energy release and decay rate vary significantly in space and time in each aftershock sequence in apparent agreement with the stress distribution following the mainshock and probably with mechanical characteristics of the fault zone. In light of these observations, it is conceivable that overall aftershock generation correlates with tectonic characteristics such as rheology, thickness, age, among others.

The hypothesis that aftershocks sequences are related to the stress distribution and conceivably to the mechanical characteristics of the fault zone, has been put to test to some extent (e.g. Drakatos and Latoussakis, 2001; Enescu et al., 2011; Henry and Das, 2001; Singh and Suarez, 1988; Tsapanos, 1995), these studies demonstrated that: the number of aftershocks correlated well with regions of strong and weak coupling; the difference of p values could be interpreted in terms of the degree of heterogeneity; subduction zone earthquakes had larger and more numerous aftershocks than earthquakes in other tectonic settings; lower values of b and p correlated with regions under increased stress or decreased crustal heterogeneity. All of these studies point towards a close relation between the rheology of the plate and the generation of aftershocks. The correlation between both parameters (p and b) has also been studied, for example Utsu (1961) and Yamashita and Knopoff (1987) derived a positive correlation between b and p values. However, using data from nine large Chinese earthquakes Ma et al. (1990) found a negative correlation between the two parameters. Wang (1994) later corroborated the latter from a large set of sequences mostly from Japan, China and the U.S. including a few events from other regions.

To analyze any characteristic of the aftershocks process, the first step has to be the identification or discrimination of dependent events from background seismicity. A physical or statistical relation to consistently discriminate between background events and aftershocks has not been obtained and thus we cannot, at this stage in time, unambiguously differentiate one type from the other. Several methods have been proposed to attempt solving this problem in a systematic manner, for example those by Gardner and Knopoff (1974) and Feltzer and Brodsky (2006) based on space-time window criteria, those based on the correlation of events (Baiesi and Paczuski, 2004, 2005; Zaliapin et al., 2008) and others based on the evaluation of the variability coefficient (Bottiglieri et al., 2009). Nevertheless, after careful comparison of results with a visual inspection of location and time of events in the vicinity of a mainshock, these methods still lack the resolution necessary to obtain the true aftershock data. Thus, in this study we use a two-step selection criteria based on the careful inspection of seismicity rate curves and expected aftershocks affectation areas.

Our main objective is to shed additional light into the aftershock generation process. The aim is to test whether a correlation between tectonic plate characteristics, such as age and displacement rate, with different parameters related to the aftershock generation process is observed for events along the Mexican subduction zone. If this hypothesis holds true it may imply that the aftershock generation process is tightly bound to the mechanical properties of the tectonic regions in which they develop.

The Mexican subduction regime involves underthrusting of the Rivera and Cocos plates beneath the North American (NOAM) and Caribbean plates (Fig. 1). The western end of the regime comprises the subduction of the Rivera plate under the NOAM plate. The boundary of Rivera subduction is defined by the extension of the Rivera Fracture zone towards the trench, as well as by the presence of the El Gordo graben (EGG, Fig. 2). At its westernmost edge an apparent interruption in background seismicity and an absence of bathymetric features may signal an end to the subduction process. The frequency of large and small events in this region is lower than the rest of the subduction regime to the east. This is in apparent concordance with the low subduction rate (~3.3 cm/yr) that has been determined for this boundary (DeMets et al., 2010) and with the young age (approximately 10 Ma) of the oceanic lithosphere being subducted in that region (Dewey and Suárez, 1991). An alternative point of view (Kostoglodov and Bandy, 1995), however, has also been put forward in the sense that there is no significant difference in plate velocity with its neighboring segment to the east. The EGG marks a diffuse boundary where the subduction of Cocos plate under the NOAM plate starts (Bandy et al., 1995). Increasing slip rates (6–7.4 cm/yr, DeMets et al., 2010) take place as we progress along the subduction towards the east, resulting in a greater frequency of occurrence of large (Ms > 7.0) events.

Near the intersection of the O'Gorman Fracture Zone with the trench a marked difference in tectonic environment is observed (Fig. 2). This is a transitional zone between the two main subduction trends of the Cocos plate. Several distinctive features can be observed including a change in seismicity and in the general source characteristics of large events (Singh and Mortera, 1991). East of this segment we find the zone where the Tehuantepec Fracture Zone intersects the trench. Even though the relative frequency of occurrence of large events in this region is smaller than that to the west, some events in the region have shown higher stress-drop than expected for their size (Singh and Mortera, 1991).

Following these and other observations Zúñiga et al. (1996) proposed a segmentation (Fig. 2) of the subduction regime which is the base for the seismogenic source zonation employed in risk estimates at a national level (Manual de Diseño de Obras Civiles, 2008). This segmentation is closely linked to changes in mechanical properties of the subducted plate and we use it as a basis for comparison but we also consider different alternatives in our analysis.

2. Data

We used the seismicity data from the *Servicio Sismológico Nacional* (Seismological Survey of Mexico, SSN) network for recent years (1988–2014). The base seismicity catalog was analyzed by Zúñiga et al. (2000) with the purpose of assessing the homogeneity of reporting of the national network. They found that a drastic change in operation took place soon after 1988. Before this date the routine procedures comprised the localization of a great number of earthquakes without assigning magnitude to the smaller events. This situation changed on 1988 since policy shifted towards a reduction in the number of small events located while making sure that a magnitude was assigned to the majority of events that were located. Thus, we focused on data for which homogeneity in magnitude and location procedures was warranted which meant data compiled after 1987.

We found that the events able to generate significant (i.e. detected at a regional level) aftershock sequences in the region had $M_w \geq 5.6$. In order to make meaningful comparisons, however, we considered only tectonically similar events, based on their focal mechanism (thrust type) and hypocentral depth (less than 40 km). 15 events fulfilled these criteria, which provided significant results are shown in Fig. 2 and their parameters are listed in Table 1.

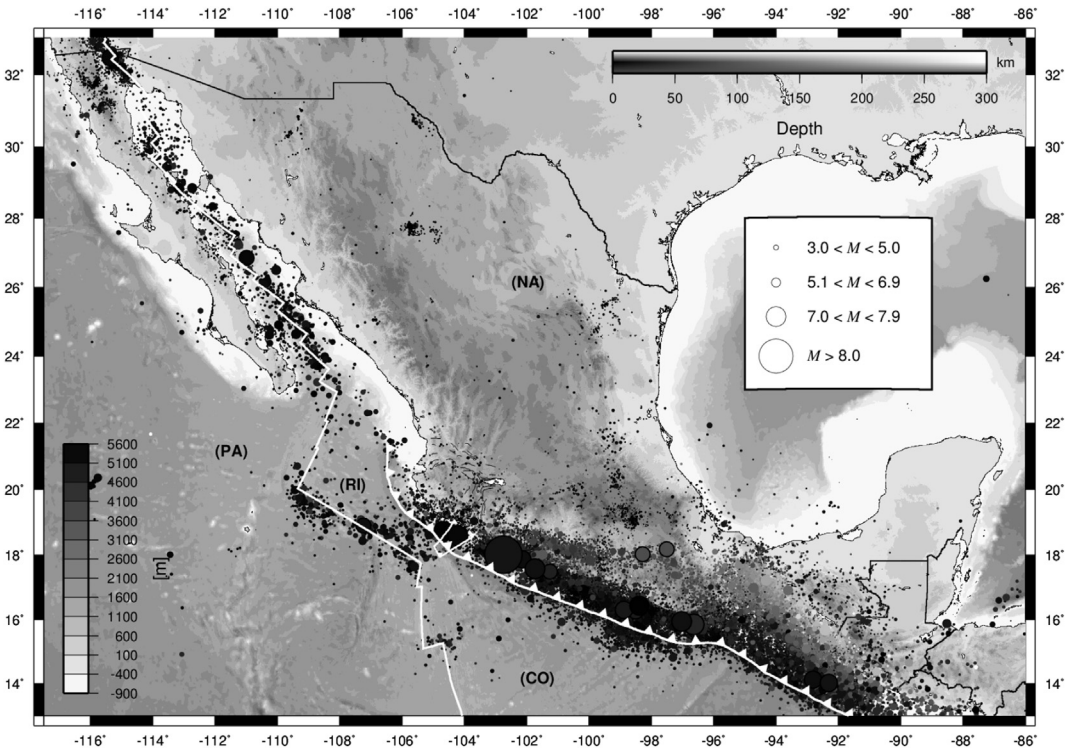

Fig. 1. Map showing the seismicity and the Mexican subduction regime, white lines represent the border of plates, circles represent earthquakes reported by the SSN from 1979 to 2013. The size of the circles is proportional to the magnitude and the color represents depth of the event. (PA)-Pacific plate, (RI) – Rivera plate, (NA) – North America plate, (CO) – Cocos plate.

3. Method

3.1. Aftershock sequence identification and analysis

Several automated procedures for the discrimination of aftershocks from background events have been proposed (e.g. Kagan and Jackson, 1991; Knopoff, 2000; Knopoff and Gardner, 1974; Molchan and Dmitrieva, 1992; Reasenberg, 1985; Zaliapin et al., 2008). However, in the case of regional data in Mexico, they fail to identify all aftershocks, which can be pointed out as dependent on the mainshock process after looking at the individual time and location of these events. This is due to the small amount of aftershocks generated by the mainshock which is an inherent characteristic of the region. In this analysis we identified aftershock sequences for each of the mainshocks of Table 1 by a two-step discrimination method based on a careful revision of the spatio-temporal situation of each sequence.

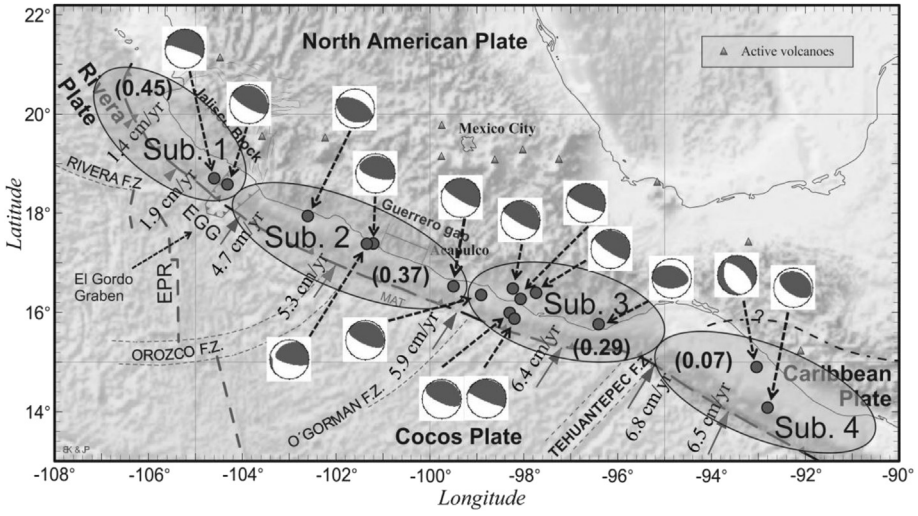

Fig. 2. Study zone (modified from Kostoglodov and Pacheco, 1999) showing epicenters of events analyzed (filled dots), focal mechanisms and main tectonic features Rivera F. Z.- Rivera fracture zone, EGG.- El Gordo Graben, Orozco F. Z.- Orozco fracture zone, O'Gorman F. Z.- O'Gorman fracture zone, Tehuantepec F. Z.- Tehuantepec fracture zone. Trench is shown by the light dashed line. Large ellipses are seismotectonic regions following a proposed segmentation of the Mexican subduction margin (Zúñiga et al., 1996), number in parenthesis indicate the coupling coefficient for each region.

Table 1
Parameters of earthquakes used for this study, aftershocks sequences, p and b values with their uncertainties and segment which belong each event.

Year	Month	Day	Latitude	Longitude	Mw	Depth	Segment	# aftershocks	p value	b value
1995	10	9	18.74	−104.67	8	15	SUB1	60	1.04 ± 0.11	1.34 ± 0.2
2003	1	22	18.6	−104.22	7.5	9	SUB1	92	0.86 ± 0.07	0.694 ± 0.08
2000	8	9	17.99	−102.66	6.5	16	SUB2	24	0.98 ± 0.12	0.655 ± 0.2
2004	1	1	17.59	−101.36	6	27.3	SUB2	20	0.7 ± 0.12	0.86 ± 0.23
2014	4	18	17.18	−101.19	7.2	10	SUB2	200	0.72 ± 0.06	1.37 ± 0.2
1989	4	25	16.53	−99.46	6.9	10	SUB2	38	0.73 ± 0.15	1.13 ± 0.3
1995	9	14	16.31	−98.88	7.3	22	SUB3	33	0.89 ± 0.33	0.827 ± 0.2
1997	7	19	15.86	−98.35	6.7	5	SUB3	51	0.89 ± 0.08	0.843 ± 0.1
1996	2	25	15.83	−98.25	7.1	3	SUB3	80	0.85 ± 0.11	0.88 ± 0.1
2012	3	20	16.49	−98.23	7.4	20	SUB3	390	0.56 ± 0.11	0.94 ± 0.09
2004	6	14	16.22	−98.16	5.6	10	SUB3	57	0.67 ± 0.06	1.8 ± 0.77
2010	6	30	16.4	−97.78	6.3	20	SUB3	113	0.54 ± 0.06	1.84 ± 0.41
1998	2	3	15.69	−96.37	6.3	33	SUB3	57	0.77 ± 0.06	1.16 ± 0.2
2012	1	21	14.87	−93	6.2	45	SUB4	148	0.74 ± 0.07	1.53 ± 0.36
1993	9	10	14.14	−92.82	7.2	14	SUB4	55	0.76 ± 0.14	1.42 ± 0.3

As a first step, we defined the aftershock influence region as a spherical volume around the mainshock, with a radius that corresponds to the maximum aftershock affectation area, following the empirical relation of Kagan (2002):

$$r_m = 20 \times 10^{(m-6)/2}\ km. \tag{3}$$

In this relation r_m is the radius of the maximum aftershock affectation area and m is the magnitude of the mainshock. Of course, real aftershock volumes depend on focal mechanism and tectonic environment among others factors and are not, in the general case, spherical, as implied by this equation. However, Kagan's (2002) relation allows us to make a first order discrimination based on the maximum distance we expect aftershocks to occur. A relation such as this imposes fewer restrictions and has lower degrees of freedom than other relations, which are dependent on additional earthquake source parameters for which we have little certainty. Such relation would be overestimating the affectation distance if we assume an elliptical distribution related to the aspect ratio of the main rupture. However, the proceeding temporal discrimination step helps narrowing the volume to a more realistic one. In general, most automated algorithms (e.g. Knopoff, 2000; Reasenberg, 1985; Zaliapin et al., 2008) rely on these two steps but constraints imposed by the algorithms generally cause losing much of the aftershock data that otherwise can be used, which in the case of Mexico is crucial due to the low productivity rate of aftershocks (Singh and Suarez, 1988).

As the second step of the analysis we further refined the data selection by a temporal window following the occurrence of the mainshock and ending at the time where the background seismicity rate for the region is resumed, thus rejecting those events that on this basis are not related to the main rupture process. We accomplish this by looking at those events occurring after the mainshock within the maximum affectation region and then selecting the time span in the cumulative number–time curve during which the highest seismicity rate (steepest slope) takes place (in most cases less than three months, Fig. 3) until the time when background rates where resumed. The evaluation of the background seismicity rate for each of the regions analyzed was carried out for those time intervals not involving a major event. The corresponding background rates and time intervals thus determined were (calculated as number of events with M $\geq$ 3.0 per year): for Sub1, 5.3 ± 2.7 (1998–2011); for Sub2, 48 ± 15.8 (2006–2012); for Sub3, 79.2 ± 11.6 (1999–2008); and for Sub4, 92.6 ± 26.2 (2003–2011).

We estimated the b values of the Gutenberg–Richter distribution for each sequence by maximum likelihood (Aki, 1965):

$$b = \frac{\log(e)}{\langle M\rangle - (M_c - \Delta M_{bin}/2)} \tag{4}$$

where $\langle M\rangle$ is the mean magnitude of the sample and $\boldsymbol{\Delta M_{bin}}$ is the binning width of the catalog (Bender, 1983; Utsu, 1999), here taken as 0.1. The minimum magnitude (M_c) was calculated by means of the maximum curvature technique of Woessner and Wiemer (2005). Uncertainties were calculated by the Shi and Bolt (1982) method. It is well known that the dependence of b on M_c is far from negligible (Wiemer and Wyss, 2000). We tried other alternate techniques for determining M_c, including the "entire magnitude range" or EMR technique of Woessner and Wiemer (2005) but results from these analyses gave larger uncertainties for our data.

Omori–Utsu p values from Equation (1) were determined by least squares fit to the temporal decay of the aftershock rate as provided by the code Zmap (Wiemer, 2001). Uncertainties in p are derived from the regression. b and p values for each sequence and their uncertainties are listed in Table 1. Fig. 3 shows an example of the selection criteria as well as the b and p value fits for the largest event analyzed.

3.2. Seismic coupling

We calculated the seismic coupling coefficient (χs) for the segments previously described (Fig. 2). This coefficient is defined as the ratio between the seismic slip rate ($\dot{u}_s$) and the slip rate derived from global plate models ($\dot{u}_m$) (Pacheco et al., 1993). The seismic slip rate for a given rectangular subduction segment with N shallow thrust interplate earthquakes over a specific period of time (T) can be expressed as

$$\dot{u}_s = \sum_{i}^{N} \frac{M_0^i}{\mu LWT}, \tag{5}$$

where μ is the rigidity, L is the length of the segment, W is the downdip width of the seismogenic zone, and Mo is the seismic moment released by an individual earthquake (Brune, 1968; Pacheco et al., 1993). We defined the seismogenic zone dimensions along the subduction zone using the 100 °C and 350 °C isotherms based on the thermal models of Currie et al. (2002) and Manea and Manea (2006) (Fig. 4). We assumed a rigidity of 4×10^{10} N/m^2 following Scholz and Campos (2012), considering events with Mw $\geq$ 5.5 reported in the global CMT catalog from 1976 to 2014. This magnitude cutoff was applied to assure a good determination of depth and focal mechanism (Pacheco et al., 1993).

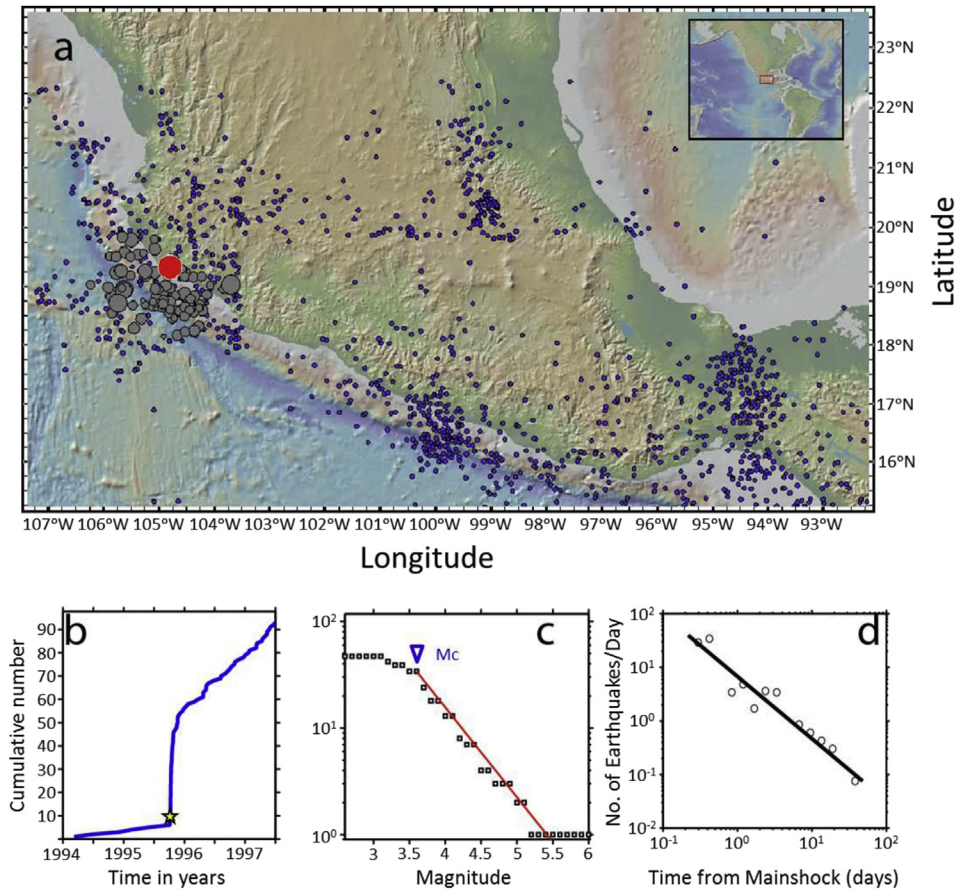

Fig. 3. a) Map showing the aftershock distribution (large gray circles) for the Colima earthquake of October 9, 1995 (Mw = 8.0), after selection process as described in the text. Background seismicity is shown for the period 1995 to 1997 for illustration purposes. b) Aftershock temporal sequence, only events within the maximum affectation area are displayed. c) Frequency-magnitude distribution and *b* value fit. d) Aftershock temporal decay and *p* value fit. Largest circle is the main event.

The convergence rates along the Mexican subduction zone were taken from the Nuvel 1 model of DeMets et al. (1990). In the Sub1, Sub2, Sub3 and Sub4 regions, the convergence rate varies in the following intervals: 1.4–1.9 cm/yr, 4.7–5.9 cm/yr, 6.4 cm/yr and 6.8–6.5 cm/yr, respectively (Fig. 2).

4. Results

In order to test the hypothesis that aftershock parameters are related to tectonic environment our results were correlated with a first order segmentation of the Mexican subduction margin (Zúñiga et al., 1996). This segmentation (Fig. 2) was defined on the basis of several key parameters: tectonic features, focal mechanism and/or faulting patterns, type of energy release (i.e. stress drop), source characteristics (i.e. simple or complex source time functions) as well as the seismic history of each region. Nevertheless, the results presented here are also of help in justifying the proposed segmentation as discussed below.

Fig. 5 shows the results of the *p* and *b* evaluation as well as plate age and slip rate as a function of longitude. The *p* values displayed in Fig. 5a indicate a maximum ($p = 1.04$) which corresponds to the October 9 1995, $M_w = 8.0$, Colima event (Fig. 3, Table 1) for which we identified an aftershock sequence of 60 events with $M_c \geq 2.0$. The minimum value ($p = 0.63$) was obtained for the May 15 1993, $M_w = 6.0$, Guerrero event (Table 1). It is important to mention that in our analysis we included an event which takes place in the diffuse intersection of the Rivera Fracture Zone with the East Pacific Rise (May 1st, 1997, $M_w = 6.9$, but does not belong to subduction regimes Sub1) since this boundary has not been reliably defined. The results of Figs. 5a and 6 indicate a slight tendency for *p* values to decrease from west to east. Uncertainties are not negligible, and show similar values except for a couple of events, which we discuss later together with a statistical significance test to corroborate this observation. It is worthwhile noticing that *p* values west of the O'Gorman Fracture Zone (i.e. segments SUB1 and SUB2 which includes the Guerrero Gap), have an average *p* of 0.84 ± 0.15 while those to the east of that longitude have an average of 0.74 ± 0.13 (Table 2). This is in an inverse relation to the plate slip rate and age (Fig. 5c) as determined from parameters from DeMets et al. (2010). Although uncertainties are somewhat large due to the small number of aftershocks in the sequences (Table 1), the uncertainty envelope confirms a decreasing trend towards the east (Fig. 6).

The *b* values calculated (Figs. 5b and 6), on the other hand, indicate a reverse trend to that of the *p* values. The maximum value (1.84) was determined for the June 30 2010, $M_w = 6.3$, Oaxaca event (Table 1) but its uncertainty (0.41) exceeds a reliable range and was not included in the statistical analysis. The minimum (0.655) was observed for the event of August 9, 2000 ($M_w = 6.5$) in Michoacan. We notice that the event localized off the Colima coast near the border between regions SUB1 and SUB2 shows an anomalous value ($b = 1.34$) with respect to the general trend. Nevertheless, we cannot discard the possibility of a small bias due to the low density of stations of the SSN network for that area of the country. However, the resolution is enough to warrant reliable estimates of *p* and *b* values. The envelope of uncertainty in *b* values (Fig. 5b), calculated by the Shi and Bolt (1982) method, confirms the increasing

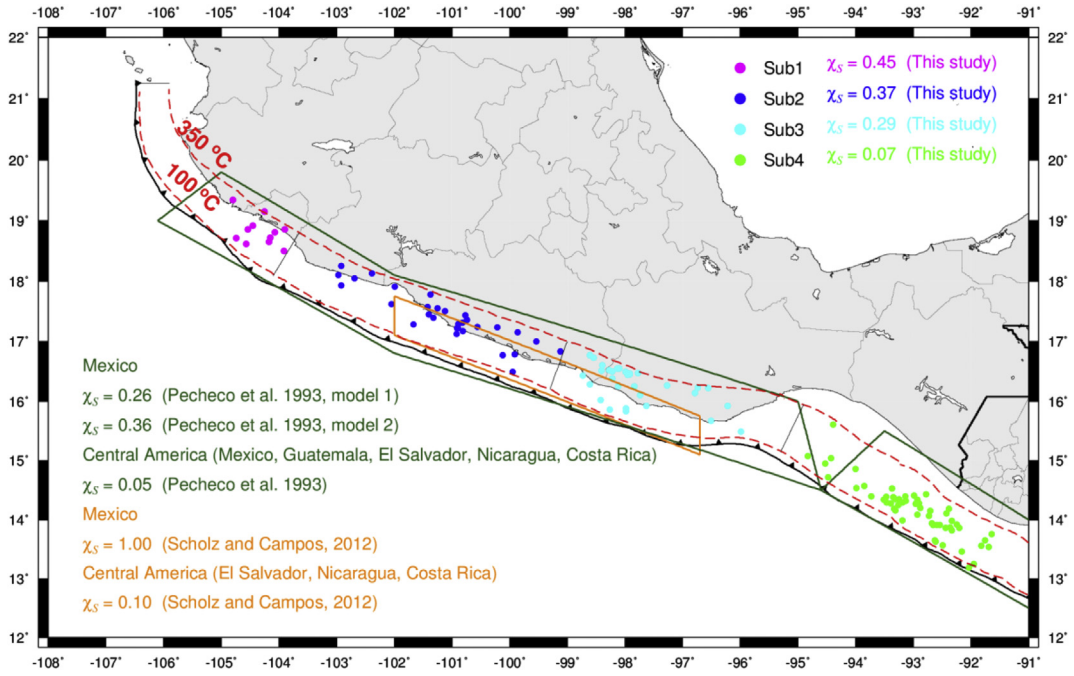

Fig. 4. Color dots are earthquake epicenters with Mw > 5.0 reported in the global CMT catalog from 1976 to 2014. The colors also indicate the segmentation of the Mexican subduction zone used in this study (Sub1, Sub2, Sub3, and Sub4 regions). Red dashed lines show the 100 °C and 350 °C isotherms used to define the seismogenic zone based on the results of Currie et al. (2002) and Manea and Manea (2006). Green irregular polygons show the seismogenic zone defined by Pacheco et al. (1993) for Mexico and Central America. Orange irregular polygon shows the seismogenic zone defined by Scholz and Campos (2012) for Mexico. χs indicates seismic coupling coefficients for each model and region including this study. (For interpretation of the references to colour in this figure legend, the reader is referred to the web version of this article.)

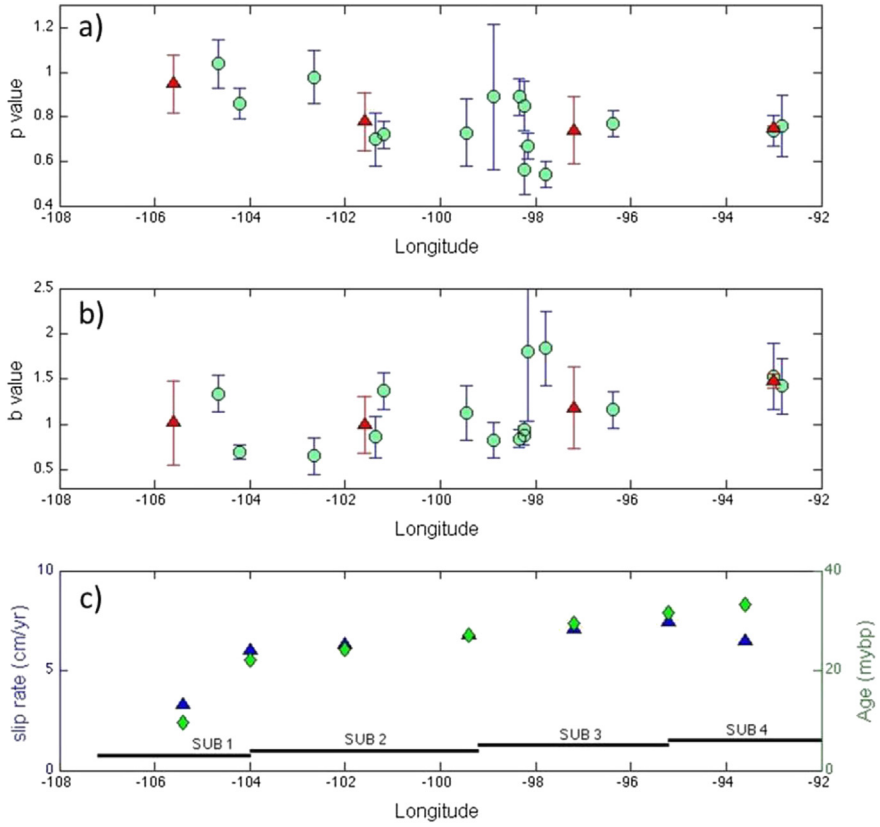

Fig. 5. a) *p* values and their uncertainty as a function of longitude. Circles are individual values and triangles are segment averages. b) *b* values and their uncertainty as a function of longitude. Segment averages as in a) are also shown. c) Plate slip rate (triangles) and age (diamonds) as a function of longitude after the model of DeMets et al. (2010). Black horizontal lines indicate the approximate extent for each segment of the subduction regime.

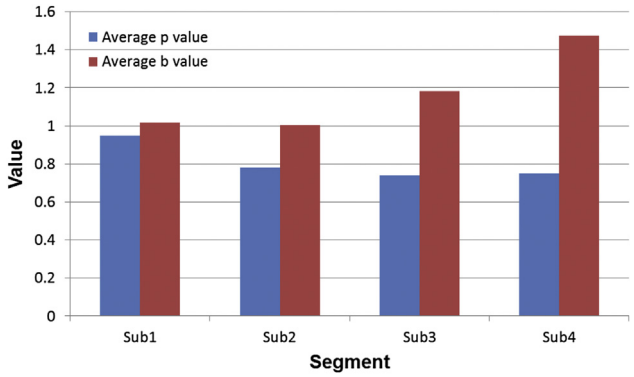

Fig. 6. Average of p and b values as a function of segment.

Table 3
Probability for the difference of the means of p *value* among segments.

	Sub2	Sub3	Sub4
Sub1	0.10	0.06	0.08
Sub2		0.33	0.39
Sub3			0.54

Table 4
Probability for the difference of the means of b *value* among segments.

	Sub2	Sub3	Sub4
Sub1	0.52	0.34	0.15
Sub2		0.25	0.06
Sub3			0.20

Table 2
Number of sequences per region, p and b values average and average depth for each segment.

Segment	No. of sequences p, b	Average p value	Average b value	Average depth	Average p Sub1&Sub2 Sub3&Sub4	Average b Sub1&Sub2 Sub3&Sub4
Sub1	2,2	0.95 ± 0.13	1.02 ± 0.46	12 ± 4	0.84 ± 0.15	1.01 ± 0.32
Sub2	4,4	0.78 ± 0.13	1.00 ± 0.31	15.8 ± 4		
Sub3	7,7	0.74 ± 0.15	1.18 ± 0.45	16.1 ± 11	0.74 ± 0.13	1.25 ± 0.41
Sub4	2,2	0.75 ± 0.01	1.48 ± 0.08	29.5 ± 22		

trend. The correlation agrees with that found by Guo and Ogata (1997) for interplate events although the regression line slope (−0.18) (Fig. 7) is quite smaller than that found by those authors (−0.706). This difference may be explained by the small number of aftershocks events (15) compared against those of other regions (Guo and Ogata, 1997). We consider that with a larger number of events, the results may be improved. However, the obtained correlation corroborates that the variability of static frictional strength changes along of subduction zone regime increasing from west to east (Guo and Ogata, 1997; Mikumo and Miyatake, 1979).

In order to test the significance of the variation of the aftershock parameters as a function of longitude we performed a statistical one-tail t test on the difference of the average of p and b values of each segment. Tables 3 and 4 show the probability of the difference in p and b, which can be directly compared to a significance level. As it is standard in these tests, values of probability lower than a predefined significance (e.g. 0.05 for 95% confidence) would indicate that the difference is significant at that confidence level. As Table 3 shows, the differences in p are statistically significant at the 90% confidence level when comparing segment SUB1 against SUB2, with 94% and 92% significance when compared to SUB3 and SUB4 respectively. The probabilities of all other tests do not allow for any significant difference, so we cannot reject the null hypothesis for all other comparisons. As to the b values, significant differences segment-wise is attained to the 94% confidence level when comparing SUB2 vs SUB4. All other tests fail to reject the null hypothesis.

If we merge the results of SUB1 with SUB2 and compare them to the merged results of SUB3 with SUB4, we obtain a probability for the difference of p values of 0.10 which is significant at the 90% confidence level. On the other hand, the probability of the difference in b values is obtained as 0.12, which corresponds to a significance no better than 88% (Table 5), indicating poor significance.

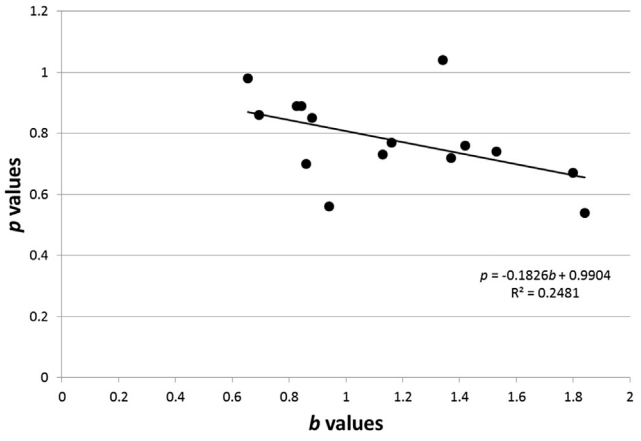

Fig. 7. p Values against the respective b values for the aftershock sequences analyzed. The least squares linear regression relation is shown as a dashed line and the resulting linear fit is shown in the box with its correlation coefficient.

5. Discussion

Table 2 includes the average p values, the number of sequences analyzed per region, uncertainties and average depth for each of the segments. Wiemer and Katsumata (1999) observed that p values can also be related to geological features so this possibility cannot be ruled out since there is evidence that the southern coastal regions of Mexico comprise an accretion of geological terranes (e.g. Keppie, 2004) and more observations are needed to clarify the issue. As they stand, we assume that aftershocks occur along the plate interface. The depths of the events do not vary significantly, hence the results do not indicate a dependence with depth due to that the most of hypocenters take place in the first 20 km of depth and their locations are in the interface between Cocos and NOAM where the plates are strongly coupled (at surface

Table 5
Probability for the difference of the means of p and b values between the western-most and eastern-most regions.

	Sub1-Sub2 vs. Sub3-Sub4
p value	0.10
b *value*	0.12

can extend to 10 Km inland from the coast, Pardo and Suárez, 1995; Pérez-Campos et al., 2008).

Results of Table 2 as displayed in Fig. 5 indicate that the change in p values in segments Sub1 and Sub2 can be related to the diffuse transition between Rivera and Cocos plates. Another change in plate age within segment Sub2 appears to also correlate with a change in both p and b values (Fig. 5). We also observe that the Guerrero Gap coincides with this transition zone. A model based on fault heterogeneity that supports the hypothesis of an inverse relation between p and b values has been proposed by Kisslinger and Jones (1991) and Wang (1994) among others.

We find seismic coupling ratios of: 0.45, 0.37, 0.29, and 0.07 for the segments Sub1, Sub2, Sub3 and Sub4, respectively (Figs. 2 and 4). The Sub1 region has the highest coefficient due to the inverse relationship between the seismic coupling and the convergence rate. These results are congruent with those reported earlier by Pacheco et al. (1993) in the sense that seismic coupling decreases towards south (Fig. 4). In their study, they obtained coefficient values ranging from 0.36 to 0.26 for a region that includes the segments Sub1, Sub2, and Sub3, and coupling coefficient of 0.05 for Central America (this region includes the segment Sub4). Scholz and Campos (2012), on the other hand, determined the seismic coupling coefficients for Mexico and Central America obtaining values of 1.0 and 0.1, respectively (Fig. 4).

The estimates of seismic coupling differ due to the use of different input parameters in Equation (5). For example, Pacheco et al. (1993) and Scholz and Campos (2012) used different rigidity values: 5×10^{10} N/m^2 and 4×10^{10} N/m^2, respectively. The time intervals are also different. For instance, Pacheco et al. (1993) used data from 1900 to 1990; Scholz and Campos (2012) from 1890 to 2012 and while in this study from 1976 to 2014. The dimensions of the seismogenic zone vary greatly in previous studies (Fig. 4). Pacheco et al. (1993) proposed two models for the seismogenic zone in Mexico. The first model with L = 1130 km and W = 89 km and the second one with a length and width of 1130 km and 65 km, respectively. On the other hand, Scholz and Campos (2012) defined the seismogenic zone with L = 550 km and W = 50 km. The convergence rate also plays an important role in the estimation of the seismic coupling. From the Nuvel 1 model (DeMets et al., 1990), we can observe significant differences in the convergence rate along the subduction zone. This highlights the importance of incorporating detailed estimates of the convergence rate in seismic coupling calculations. The differences could result from inaccurate convergence rate values. Pacheco et al. (1993) used an average convergence rate of 6.0 cm/yr for the regions Sub1, Sub2, and Sub3 while Scholz and Campos (2012) used a value of 5.7 cm/yr for the regions Sub2, and Sub3.

Our results suggest a strong coupling for the western part which follows the high p and low b values, in contrast to eastern part where the seismic coupling is weak and p values are low while b values are higher. This is in agreement with the results of Singh and Suarez (1988), since they conclude that aftershock generation is related with the level of coupling. The observed low number of aftershocks in the Mexican subduction regime, as compared to other subduction regimes, has a mild correlation with the degree of coupling along the young plate interface (Singh and Suarez, 1988). This indicates that the tectonic setting may control aftershock generation. The p values found in our study have a slight tendency to decrease from west to east in a direct relation with plate age and thus with the temperature of the lithosphere. The opposite is observed in the case of b values, since, in general, the lowest values were obtained at the western end and the largest towards the east, although the significance of the change is not enough to warrant that the effect is real.

The p and b values are slightly correlated with a first order segmentation proposed by Zúñiga et al. (1996) which in general terms also depends on tectonic characteristics. b values have been found to be usually large for events that do not show a significant rupture heterogeneity (Enescu and Ito, 2002) as is the case for the region (SUB4) at the eastern end of the subduction regime, while the opposite would be expected for events towards the western end. The significance of the eastward decreasing variation in p values is enough to accept it at the 90% confidence level when comparing the merged results of the two western-most regions (SUB1 and SUB2) to the two eastern-most regions (SUB3 and SUB4). A significance better than 88% is calculated for the eastward increasing trend in b value, when comparing the merged results of the two western-most regions (SUB1 and SUB2) to the two eastern-most regions (SUB3 and SUB4). Individual regional tests fail to reject the null hypothesis except for the comparison of SUB1 p values against all other regions. In the case of b values significant differences segment-wise is attained to the 94% confidence level when comparing SUB2 vs SUB4. All other tests fail to reject the null hypothesis.

An inverse relation between the trend of p values and that of the b values, although apparent, is not statistically significant. Nevertheless, the results should encourage further investigation into the matter since the small number of regionally detected aftershocks of the sequences (a natural condition of the Mexican subduction regime) could be precluding better significance. Our results are consistent with the results of Ma et al. (1990) for large earthquakes in China which also found a negative correlation between the two parameters. Wang (1994) also corroborated the latter from a large set of sequences mostly from Japan, China and the U.S. including a few events from other regions.

The eastern part of the Mexican subduction regime would conceivably have a larger seismic hazard due to aftershocks occurrence since they take more time to decay (low p values). Moreover, higher aftershock b values at the eastern end indicate a larger ratio of strong vs. moderate earthquakes which may also have an adverse effect on risk of damage to structures, being subjected to larger events after a mainshock. These results are correlated to the degree of coupling between the subducting and overriding plates by means of the seismic coupling coefficient found for each region, since we found that the western part shows a strong coupling (where high p values and low b values were obtained) while the eastern part shows a weak coupling (with low p values and high b values).

6. Conclusions

We found somewhat higher aftershock b values at the eastern end of the Mexican subduction regime indicating a larger ratio of strong vs. moderate earthquakes. These results are correlated to the degree of coupling between the subducting and overriding plates by means of the seismic coupling coefficient found for each region, since we found that the western part shows a strong coupling (where high p values and low b values were obtained) while the eastern part shows a weak coupling (with low p values and high b values). Overall, with current data from the Mexican subduction regime we cannot statistically confirm the hypothesis that aftershock generation depends on certain tectonic characteristics (age, thickness, temperature). Nevertheless, our results do not reject the hypothesis either, thus encouraging further study into this question. Recently, Nishikawa and Ide (2014) observed that b value correlates with age of plate in a global study. Both ours and Nishikawa and Ides's results support the observation of b value dependence with age of the plate. There are enough indications that the apparent trend in both b and p values is a reflection of the

tendency of the plate to increase in age (and thus in thermal properties) at the subduction regime as we progress towards the East. The small variation observed may be due to the fact that even though the plate undergoes a change in age as it subducts, its effect in thermal properties may not be as large.

Acknowledgments

The authors wish to thank the reviewers whose comments helped us to clarify our methodology and provided helpful suggestions for presenting and discussing our results. We also wish to thank the personnel of *Servicio Sismológico Nacional* (Seismological Service of Mexico, SSN) who are in charge of the national seismic network. In particular, we would like to acknowledge Casiano Jimenez's work in keeping the seismicity catalog up to date. The SSN is operated by the Institute of Geophysics, UNAM. This work was partially funded by grants IN122602 and IN108115 from UNAM DGAPA/PAPIIT program. LAB and QRP work is funded through CONACyT Cátedras program (2602 and 1126 respectively), which is gratefully acknowledged.

References

Aki, K., 1965. Maximum likelihood estimate of b in the formula $\log N = a\ bM$ and its confidence limits. Bull. Earthq. Res. Inst. 43, 237–239.
Baiesi, M., Paczuski, M., 2004. Scale-free networks of earthquakes and aftershocks. Phys. Rev. E 69, 066106. http://dx.doi.org/10.1103/PhysRevE.69.066106.
Baiesi, M., Paczuski, M., 2005. Complex networks of earthquakes and aftershocks. Nonlinear Process. Geophys. 12, 1.
Bandy, W., Mortera-Gutierrez, C., Urrutia-Fucugachi, J., Hilde, T.W.C., 1995. The subducted Rivera-Cocos plate boundary: where is it, what is it, and what is its relationship to the Colima rift? Geophys. Res. Lett. 22, 3075–3078.
Bender, B., 1983. Maximum likelihood estimation of b values for magnitude grouped data. Bull. Seismol. Soc. Am. 73, 831–851.
Bottiglieri, M., Godano, C., D'Auria, L., 2009. Distribution of volcanic earthquake recurrence intervals. J. Geophys. Res. 114, B10309. http://dx.doi.org/10.1029/2008JB005942.
Brune, J., 1968. Seismic moment, seismicity, and rate of slip along major fault zones. J. Geophys. Res. 73, 777–784.
Currie, C.A., Hyndman, R.D., Wang, K., Kostoglodov, V., 2002. Thermal models of the Mexico subduction zone: implications for the megathrust seismogenic zone. J. Geophys. Res. 107 (B12) http://dx.doi.org/10.1029/2001JB000886.
DeMets, C., Gordon, R.G., Argus, D.F., 2010. Geologically current plate motions. Geophys. J. Int. 181, 1–80. http://dx.doi.org/10.1111/j.1365-246X.2009.04491.x.
DeMets, C., Gordon, R.G., Argus, D.F., Stein, S., 1990. Current plate motions. Geophys. J. Int. 101, 425–478.
Dewey, J.W., Suárez, G., 1991. Seismotectonics of Middle America. In: Slemmons, et al. (Eds.), Neotectonics of North America, vol. 1. Geological Society of America, Decade Map, pp. 309–321.
Drakatos, G., Latoussakis, J., 2001. A catalog of aftershock sequences in Greece (1971-1997): their spatial and temporal characteristics. J. Seismol. 5, 13745.
Enescu, B., Ito, K., 2002. Spatial analysis of the frequency-magnitude distribution and decay rate of aftershock activity of the 2000 Western Tottori earthquake. Earth Planets Space 54, 847–859.
Enescu, B., Enescu, D., Ito, K., 2011. Values of b and p: their variations and relation to physical processes for earthquakes in Japan and Romania. Romanian J. Phys. 56 (3–4), 590–608.
Feltzer, K.R., Brodsky, E.E., 2006. Decay of aftershock density with distance indicates triggering by dynamic stress. Nature 441, 735–738. http://dx.doi.org/10.1038/nature04799.
Gardner, J.K., Knopoff, L., 1974. Is the sequence of earthquakes in southern California, with aftershocks removed, poissonian? Bull. Seismol. Soc. Am. 64 (5), 1363–1367.
Gutenberg, B., Ritcher, C.F., 1942. Earthquake magnitude, intensity, energy and acceleration. Bull. Seismol. Soc. Am. 32 (3), 163–191.
Guo, Z., Ogata, Y., 1997. Statistical relations between the parameters of aftershocks in time, space and magnitude. J. Geophys. Res. 102 (B2), 2857–2873.
Henry, C., Das, S., 2001. Aftershock zones of large shallow earthquakes: fault dimensions, aftershock area expansion and scaling relations. Geophys J. Int. 147, 272–293.
Kagan, Y.Y., 2002. Aftershock zone scaling. Bull. Seismol. Soc. Am. 92, 641–655.
Kagan, Y.Y., Jackson, D.D., 1991. Long-term earthquake clustering. Geophys. J. Int. 104, 117–134. http://dx.doi.org/10.1111/j.1365-246X.1991.tb02498.x.
Kato, A., Arao, M., Ariyoshi, K., Asano, Y., Doi, K., Enescu, B., Fujieda, S., Hagiwara, H., Haneda, T., Hasegawa, A., Hashimoto, S., Hirahara, S., Hirata, N., Hirata, Y., Hirose, I., Hondo, S., Hori, K., Hori, S., Horiuchi, S., Igarashi, T., Iidaka, T., Iio, Y., Ikuta, R., Ito, T., Iwasaki, T., Kamimura, A., Kanazawa, T., Kano, Y., Katao, H., Kawamoto, S., Kawamura, T., Kita, S., Kobayashi, M., Kohno, Y., Kono, T., Kosuga, M., Kubo, A., Kurashimo, E., Matsumoto, S., Matsushima, T., Matsuzawa, T., Mitsui, N., Miura, R., Miyazawa, M., Mizukami, T., Murotani, S., Nagai, S., Nakajima, J., Nakayama, T., Negishi, H., Nishigami, K., Ogino, I., Ohmi, S., Okada, T., Onaha, H., Gamage, S.S.N., Saka, M., Sakai, S., Sato, K., Sato, T., Serizawa, M., Shibutani, T., Shimizu, J., Suganomata, J., Tagami, K., Takahashi, K., Takai, K., Takeuchi, F., Takumi, Y., Tanaka, K., Tatsumi, K., Tonegawa, T., Tsushima, H., Uchida, N., Uehira, K., Ueno, T., Umino, N., Wada, H., Watanabe, K., Watanabe, S., Yabe, Y., Yaginuma, T., Yamada, M., Yamamoto, S., Yamanaka, Y., Yamashita, F., Yamazaki, F., Yui, S., Yukutake, Y., 2007. High-resolution aftershock observations in the source region of the 2004 mid-Niigata prefecture Earthquake. Earth Planets Space. ISSN: 13438832 59 (8), 923–928.
Kato, A., Igarashi, T., 2012. Regional extent of the large coseismic slip zone of the 2011 Mw 9.0 Tohoku-Oki earthquake delineated by on-fault aftershocks. Geophys. Res. Lett. 39, L15301. http://dx.doi.org/10.1029/2012GL052220.
Keppie, D., 2004. Terranes of Mexico revisited: a 1.3 billion year Odyssey. Int. Geol. Rev. 46, 765–794. http://dx.doi.org/10.2747/0020-6814.46.9.765.
Kisslinger, C., Jones, L.M., 1991. Properties of aftershocks sequences in southern California. J. Geophys Res. 96, 11,947–11,958.
Knopoff, L., 2000. The magnitude distribution of declustered earthquakes in Southern California. Proc. Natl. Acad. Sci. 97 (22), 11880–11884.
Knopoff, L., Gardner, J.K., 1974. Is the sequence of earthquakes in southern California, with aftershocks removed, Poissonian? Bull. Seismol. Soc. Am. 64 (5), 1363–1367.
Kostoglodov, V., Pacheco, J., 1999. Cien años de sismicidad en México. Instituto de Geofísica, UNAM. (Poster).
Kostoglodov, V., Bandy, W., 1995. Seismotectonic constraints on the convergence rate between the Rivera and North American plates. J. Geophys. Res. 100, 17,977–17,989.
Ma, Z., Fu, Z., Zhang, Y., Wang, C., Zhang, G., Liu, D., 1990. Earthquake Prediction, Nine Major Earthquakes in China (1966–1976), Seismological Press Beijing. Springer, New York, p. 332.
Manea, V.C., Manea, M., 2006. Origin of the Modern Chiapanecan Volcanic Arc in Southern Mexico Inferred from Thermal Models. Geological Society of America, pp. 27–38. http://dx.doi.org/10.1130/2006.2412(02). Special Papers 2006, 412.
Manual de Diseño de Obras Civiles. Diseño por Sismo, 2008. Comisión Federal de Electricidad. Instituto de Investigaciones Eléctricas, México.
Mikumo, T., Miyatake, T., 1979. Earthquake sequences on a frictional fault model with non-uniform strengths and relaxation times. Geophys. J. R. Astron. Soc. 59, 497–522.
Molchan, G.M., Dmitrieva, O.E., 1992. Aftershock identification: methods and new approaches. Geophys. J. Int. 109, 501–516. http://dx.doi.org/10.1111/j.1365-246X.1992.tb00113.x.
Nishikawa, T., Ide, S., 2014. Earthquake size distribution in subduction zones linked to slab buoyancy. Nature Geosci. 7, 904–908. http://dx.doi.org/10.1038/NGEO2279.
Omori, F., 1895. On the after-shocks of Earthquakes. Coll. Sci., Imperial University 7 (2), 111–200.
Pacheco, J.F., Skyes, L.N., Scholz, C.H., 1993. Nature of seismic coupling along simple plate boundaries of subduction type. J. Geophys. Res. 98, 14,133–14,159.
Pardo, Mario, Suárez, Gerardo, 1995. Shape of the subducted Rivera and Cocos plates in southern Mexico: seismic and tectonic implications. J. Geophys. Res. 100 (B7), 12,357–12,373.
Pérez-Campos, X., Kim, Y., Husker, A., Davis, P.M., Clayton, R.W., Iglesias, A., Pacheco, J.F., Singh, S.K., Manea, V.C., Gurnis, M., 2008. Horizontal subduction and truncation of the Cocos Plate beneath central Mexico. Geophys. Res. Lett. 35, L18303. http://dx.doi.org/10.1029/2008GL035127.
Reasenberg, P., 1985. Second-order moment of Central California seismicity, 1969-1982. J. Geophys. Res. 90 (B7), 5479–5495.
Scholz, C.H., Campos, J., 2012. The seismic coupling of subduction zones revisited. J. Geophys. Res. 117, B05310. http://dx.doi.org/10.1029/2011JB009003.
Shi, Y., Bolt, B.A., 1982. The standard error of the magnitude-frequency b value. Bull. Seismol. Soc. Am. 72, 1677–1687.
Singh, S.K., Mortera, F., 1991. Source time functions of large Mexican subduction earthquakes, morphology of the Benioff Zone, age of the plate and their tectonics implications. J. Geophys. Res. 96, 21487–21502.
Singh, K.S., Suarez, G., 1988. Regional variation in the number of aftershocks ($m_b > 5$) of large, subduction zone earthquakes ($m_w > 7.0$. Bull. Seismol. Soc. Am. 78, 230–242.
Toda, S., Stein, R.S., Reasenberg, P.A., Dietrich, J.H., Yoshida, A., 1998. Stress transferred by the 1995 Mw = 6.9 Kobe, Japan, shock: effect on aftershocks and future earthquake probabilities. J. Geophys Res. 103 (24), 543–565.
Tsapanos, T.M., 1995. The temporal distribution of aftershocks sequences in the subduction zones of the Pacific. Geophys J. Int. 123, 633–636.
Utsu, T., 1961. A statistical study on the occurrence of aftershocks. Geophys. Mag. 30, 521–605.
Utsu, T., 1999. Representation and analysis of the earthquake size distribution: a historical review and some new approaches. Pure Appl. Geophys 155, 471–507.
Utsu, T., Ogata, Y., Matsuura, R.S., 1995. The centenary of the omori formula for the decay law of aftershock activity. J. Phys. Earth 43, 1–33.
Wang, J., 1994. On the correlation of observed Gutenberg-Richter's b value and Omori's p value for aftershocks. Bull. Seism. Soc. Am. 84, 2008–2011.
Wiemer, S., 2001. A software package to analyze seimicity: Z-map. Seismol. Res. Lett. 72, 373–382.
Wiemer, S., Katsumata, K., 1999. Spatial variability of seismicity parameters in aftershocks zones. J. Geophys Res. 104 (13), 13,135–13,151.

Wiemer, S., Wyss, M., 2000. Minimum magnitude of completeness in earthquake catalogs: examples from Alaska, the Western United States, and Japan. Bull. Seismol. Soc. Am. 90 (4), 859–869.

Woessner, J., Wiemer, S., 2005. Assessing the quality of earthquake catalogues: estimating the magnitude of completeness and its uncertainty. Bull. Seismol. Soc. Am., 005 95 (2), 684–698. http://dx.doi.org/10.1785/012004007.

Yamashita, T., Knopoff, L., 1987. Model of aftershock occurrence. Geophys. J. R. Astr. Soc. 91, 13–26.

Zaliapin, I., Gabrielov, A., Keilis-Borok, V., Wong, H., 2008. Clustering analysis of seismicity and aftershock identification. Phys. Rev. Lett. 101 (1), 018501. http://dx.doi.org/10.1103/PhysRevLett.101.018501 (4 pages).

Zúñiga, F.R., Suarez, G., García, V., Ordaz, M., 1996. Peligro Sísmico en Latinoamérica y el Caribe, Capíulo 2: México, p. 82. Reporte final, Seismic Hazard Project, IPGH/OEA-IDRC.

Zúñiga, F.R., Reyes, M.A., Valdés, C.M., 2000. General overview of the catalog of recent seismicity compiled by the Mexican Seismological Survey. Geofísica Int. 39 (2), 161–170.